Proceedings of the 17th IEEE International
Conference on Nano/Micro Engineered and Molecular Systems
April 14-17, 2022

Nanowell-based Nano/Micropolarizer Array Biochip for Super-Resolution Imaging

1st Hsin-Yi Hsieh
Wafer Level Optics Organization
VisEra Technologies Company Limited
Hsinchu City 30078, Taiwan
orcid.org/0000-0002-2762-8856

2nd Chung-Hao Lin
Wafer Level Optics Technology Integration
VisEra Technologies Company Limited
Hsinchu City 30078, Taiwan
orcid.org/0000-0002-8781-4976

3rd Po-Chou Chen
Wafer Level Optics Technology Integration
VisEra Technologies Company Limited
Hsinchu City 30078, Taiwan

4th Wei-Ko Wang
Wafer Level Optics Technology Integration
VisEra Technologies Company Limited
Hsinchu City 30078, Taiwan
orcid.org/0000-0002-9836-5408

5th Chin-Chuan Hsieh
Wafer Level Optics Organization
VisEra Technologies Company Limited
Hsinchu City 30078, Taiwan
jchsieh@viseratech.com

***Abstract*—The diffraction barrier of an optical system restricts the minimum resolvable pitch among neighboring reaction sites on a nano/microarray chip, to impact the throughput and the detection cost. Similar to superresolution microscopy of structured illumination microscopy (SIM), a methodology is introduced to realize a theoretical √ 2-fold resolution improvement *via* a checkerboard illumination on the nanowell array. This approach involves two-step imaging and simple equipment adaptations: (1) integration of a 0/90-degree nano/micropolarizer array in a rectangular interspaced arrangement under nanowells as a biochip and (2) insertion of an 0/90-degree-switchable polarizer plate between the excitation light and biochip. For the first imaging under 0-degree polarized illumination, only the half signals on the 0-degree-nano/micropolarizer units can be acquired; for the second imaging under the 90-degree polarized illumination after 90-degree rotation of the excitation light polarizer plate, the other half signals on the 90-degree nano/micropolarizer units can be obtained. Using a virtual distance that occurs between any two 'bright' fluorescence signals, two objects within the diffraction distance can still be visualized. We have demonstrated that a 0.9-µm pitch widefield image unresolvable *via* a 20X/NA0.5 objective can be divided into two resolvable images with sufficient signal-to-noise ratio (SNR) on the biochip with an aluminum polarizer array of 180-nm thickness, 0.9-µm pixel size, 300-nm pitch, and ~0.5 duty cycle. This method simplifies the imaging capture and deconvolution process compared to the existing SIM and provides possibilities for a miniature super-resolution microscope.**

Keywords—diffraction limit, nanoarray, micropolarizer array (MPA), structure illumination microscopy (SIM), super-resolution microscopy

I. INTRODUCTION

The minimum resolvable distance between two light beams is defined based on the Rayleigh criterion as 0.61-fold wavelength divided by the numerical aperture (NA) of an objective where the first minimum intensity of a point spread function (PSF) overlaps with the maximum intensity of the other PSF. Thanks to the advance in the semiconducting industry, the feature size of photolithography has achieved sub-100 nm for a long time. However, the array density of a fluidic chip remains ~650 nm due to the resolution limit of an optomechanical system, e.g. 20X/NA0.75 Nikon air objective with a 1-mm working distance (WD) for scanning imaging capture in Illumina HiSeq sequencer, until the upgrade of the sequencer with superresolution microscopy [1, 2].

Existing superresolution microscopy has demonstrated to reduce the diffraction barrier from ~250 nm (based on a general microscope with an oil-immersed objective) to smaller than 120 nm. SIM employs sinusoidal interference patterns, which are generated by a light passing through a grating nanostructure and re-focused the directions of the first-order diffraction beams, and multiple images captured in a linear movement and/or an angular rotation for a Fourier deconvolution to obtain 2-fold resolution improvement. The other techniques use a spatial/temporal modulation of two photoswitching transitions of a fluorophore, such as stochastic optical reconstruction microscopy (STORM), or an optical beam size reduction in the excitation illumination, such as in stimulated emission depletion (STED) microscopy [3, 4]. However, current methods only emphasize controlling the light spots assemblies on the back focal plane of an objective to generate various bright/dark interspaced patterns in either one, two, three, or four dimensions from the x-axis, y-axis, z-axis, and time domain for resolution improvement.

In this paper, we propose another possibility for the generation of the checkerboard illumination pattern direct using orthogonal oriented alumina (Al) nano/micropolarizer array [5] embedded under the nanowells as a polarized excitation light filter for interval illumination in space of nanowells to generate a virtual distance (dark spacing) among neighboring reaction sites (any two bright signals) [6, 7]. A √ 2-fold resolution improvement is demonstrated by simply adaptions on a conventional fluorescence microscope with ~10 degrees leveling and rotation angle tolerances for the optomechanics. However, the deficiency of this method is the attenuation of the signal intensity (at least a twofold decay when unpolarized excitation or emission light passes through the polarizer) and the requirement of two image capture (*via* the polarizing plate at the first (e.g., 0-degree) and second (e.g., 90-degree) angles).

978-1-6654-8301-8/22/$31.00 ©2022 IEEE

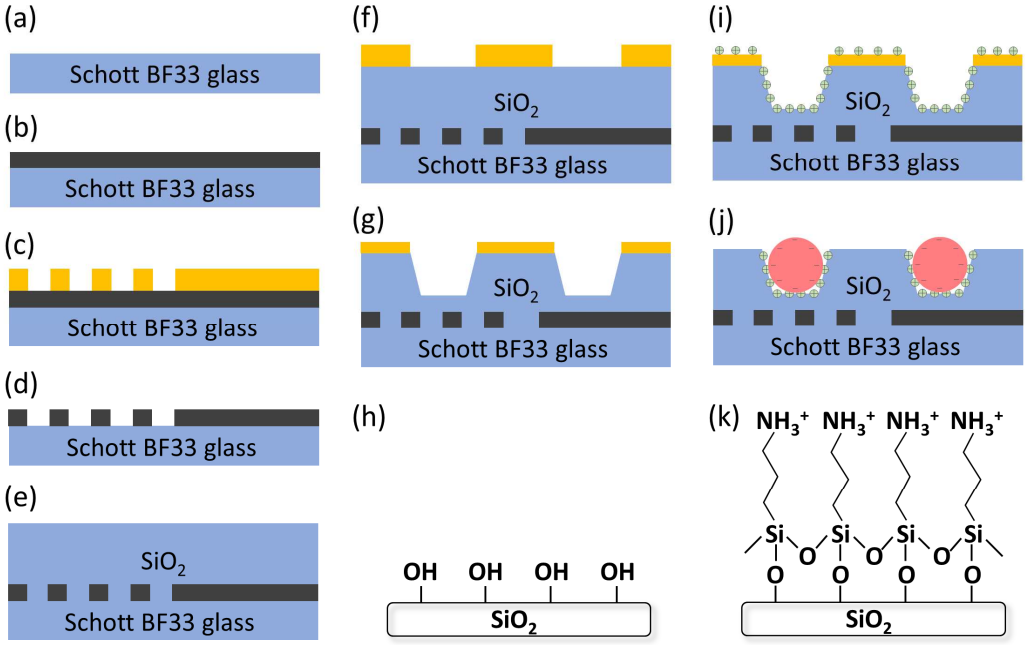

Fig. 1. Orthogonal nano/micropolarizer array biochip fabrication and surface treatment process. (a)(b) An 8" glass substrate is treated with oxygen plasma and deposited with 180-nm aluminum film. The substrate is (c) photoresist patterned by DUV photolithography and then (d) etched removed the aluminum to form polarizer array. (e) A 700-nm SiO_2 layer is deposited on the polarizer array. (f)(g) Another DUV photolithography and etching is performed to form nanowells on each sub-polarizer unit. (h)(i)(j)(k) The -OH group on the SiO_2 surface can be modified with APTES to generate a positive charge and attract negatively charged fluorescent beads in the nanowells.

II. Method and Materials

A. Materials

Polystyrene beads with a red fluorescence labeling (cat. no. R400, ex/em 542 nm/612 nm) were purchased from Thermo Scientific (USA). 3-APTES (product no. 741442) was purchased from Sigma-Aldrich (USA). BF33 borosilicate glass with a thickness of 725 µm was purchased from WaferPlus Technology (Taiwan).

B. Chip fabrication process

There were two sections on a die with each 10 mm x 20 mm area: a region includes uniform Al grating polarizer in 0-degree; and the other region includes 0-degree and 90-degree interspaced nano/micropolarizer array with four nanowell pitch sizes, ***p***, of 0.6 µm, 0.9 µm, 1.2 µm, and 1.5 µm. All the Al grating has a thickness of 180 nm, a period of 300 nm, and a duty cycle of 0.5. For the fabrication process, a 180-nm Al layer was first deposited on the oxygen-plasma-treated BF33 glass wafer (Fig. 1(a)(b)). Then, the grating structure with a 300-nm period was fabricated through DUV photolithography (FPA-5000 ES4 248 nm KrF Scanner, Canon, Japan) and etched by an AMAT DPSII etcher (DPSII Centura etcher, Applied Materials, USA) under 1200/50 W, 10 mTorr, Cl_2/CHF_3 100/10 sccm for 60 sec, and 250/50 W, $BCl_3/Cl_2/N_2/Ar$ flow 20/40/10/60 sccm for ~54 sec (Fig. 1(c)(d)). Followed by 700-nm SiO_2 deposition (Fig. 1(e)), a 450-nm nanowell array was patterned through DUV photolithography with an alignment resolution of 80 nm to the layer of the nano/micropolarizer array. Etching was performed to remove SiO_2 to a thickness of 350 nm by an AMAT DPSII etcher under 500/85 W, 80°C, 5 mTorr, $BCl_3/Cl_2/Ar$ 30/25/60 sccm for 345 sec (Fig. 1(f)(g)). The revealed surface of the SiO_2 nanowell (Fig. 1(h)) was further modified with 3-APTES (immersion in 1% APTES solution in 99.5% ethanol for 1 hr) to graft with amine groups (Fig. 1(i)). After removal of the photoresist (in acetone and ethanol solution for 10 min each under ultrasonication), loading fluorescent beads (1% 400-nm fluorescent beads diluted 1:1 with 95% ethanol), washing, and blown dry with compressed air, the negative charge fluorescent beads were attracted on the nanowell surface due to the positive charge amine groups of 3-APTES (Fig. 1(j)(k)) [8-10].

C. Optical system

An inverted microscope system (model CKX53 from Olympus (Japan)) was attached with a 530-nm high-intensity coaxial spotlight source (stock no. 11026 from Edmund Optics (USA)) before a polarizer plastic sheet (product no. P50, 50 mm x 50 mm from 3Dlens Corporation (Taiwan)) for transmission mode observation to collect the signals of a checkerboard excitation pattern on the biochip *via* an MPLN50X/NA0.75 objective on the opposite side of the chip (refer to Fig. 2(a), but without the excitation light rejection filter before the detector). For reflection mode observation of fluorescent beads in nanowells (Fig. 2(b)), the microscope was using its UV light source (ULH100HG) passing through a wire grid polarizer glass (stock no. 12647, 50 mm x 50 mm from Edmund Optics (USA), a fluorescence filter cube (U-MWG), and a UPLFLN20X/NA0.5 objective to irradiate the excitation light on the beads loaded biochip, and the fluorescence signals were collected at the same side of the chip. The Grasshopper3 USB3 camera (model no. GS3-U3-15S5C-C; 1.5MP, 45 fps, SONY ICX825) was purchased from FLIR System, Inc. (USA) as the detector. Besides, the P50 polarizer plastic sheet was used in front of a monochromator (Model MFS-630 from Hong-Ming Technology Co., Ltd. (Taiwan)) to generate polarized light and measure the TM transmittance, TE transmittance, and the extinction ratio of the fabricated 10 mm x 20 mm Al polarizer plate.

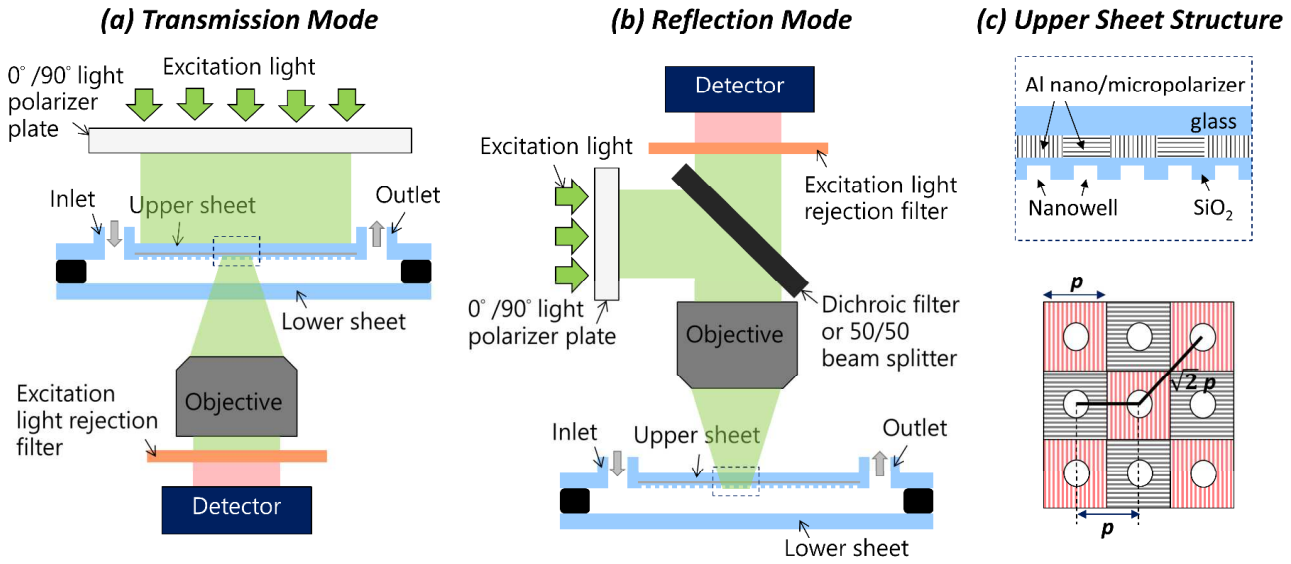

Fig. 2. Schematic illustration of the optical systems and the nanowell-based orthogonal nano/micropolarizer array biochip. (a) In transmission mode, the excitation light is polarized in either 0 or 90 degrees to irradiate on the biochip and collect the fluorescence signals on the other side of the biochip. (b) In reflection mode, the excitation light is polarized in either 0 or 90 degrees to irradiate on the biochip and collect the fluorescence signals at the same side of the biochip. (c) The upper sheet structure of the biochip is designed to embed with an orthogonal nano/micropolarizer array under the nanowells.

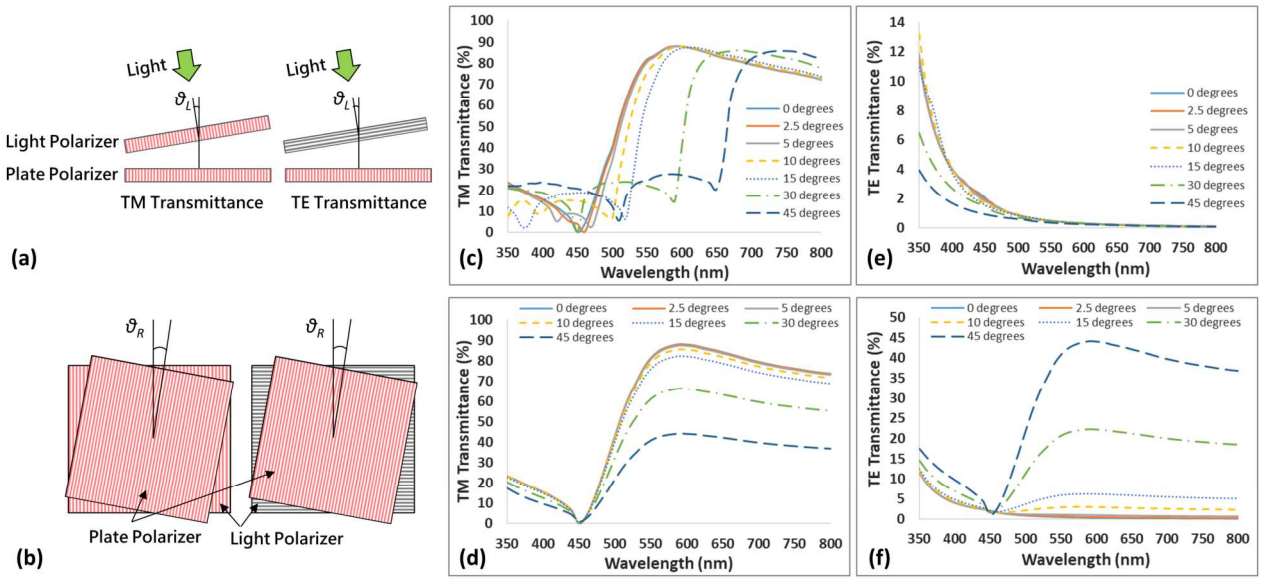

Fig. 3. Simulation of the optical property of two polarizers for the leveling and rotation tolerance. Schematic illumination of two polarizers with (a) leveling angle shift and (b) rotation angle shift. (c)(d) The TM spectrum and (e)(f) TE transmittance of the two polarizers under leveling angle shift and rotation angle shift conditions, respectively.

D. Extinction ratio and SNR calculation

The extinction ratio was the maximum transmitted intensity (TM transmittance through two polarizers with the same polarization orientation) divided by the minimum intensity (TE transmittance through two polarizers with 90 degrees angle shift). The exSNR was calculated as the ratio of the average excitation light intensity of those pixels with the maximum transmitted intensity to the standard deviation of the background of those pixels with the minimum transmitted intensity. After bead loading and image capture *via* excitation/emission of 545±15 nm bandpass/580 nm longpass filters in the U-MWG filter cube, the emSNR was calculated as the ratio of the average emission light intensity of those pixels with bright intensity (on either the five nanowells above the vertical polarizing units or the four nanowells above the horizontal polarizing units) to the standard deviation of the background region in a 3 x 3 array (Fig. 2(c)).

E. Simulation of polarizer alignment tolerance

The working principle of this method is based on the angle switch of the excitation light polarizer plate between 0 and 90 degrees to irradiate 0-degree or 90-degree polarized excitation light on the nanowells through the 0/90-degree nano/micropolarizer array. For each angle (0-degree or 90-degree) of the excitation polarizer, only the fluorophores in reaction sites on the nano/micropolarizer units with the same polarization angle can be excited for emitting the fluorescent signals. The included angle between the orientation of the excitation polarizer plate and the nano/micropolarizer will affect the optical performance of the checkerboard illumination, so the included angles between the two

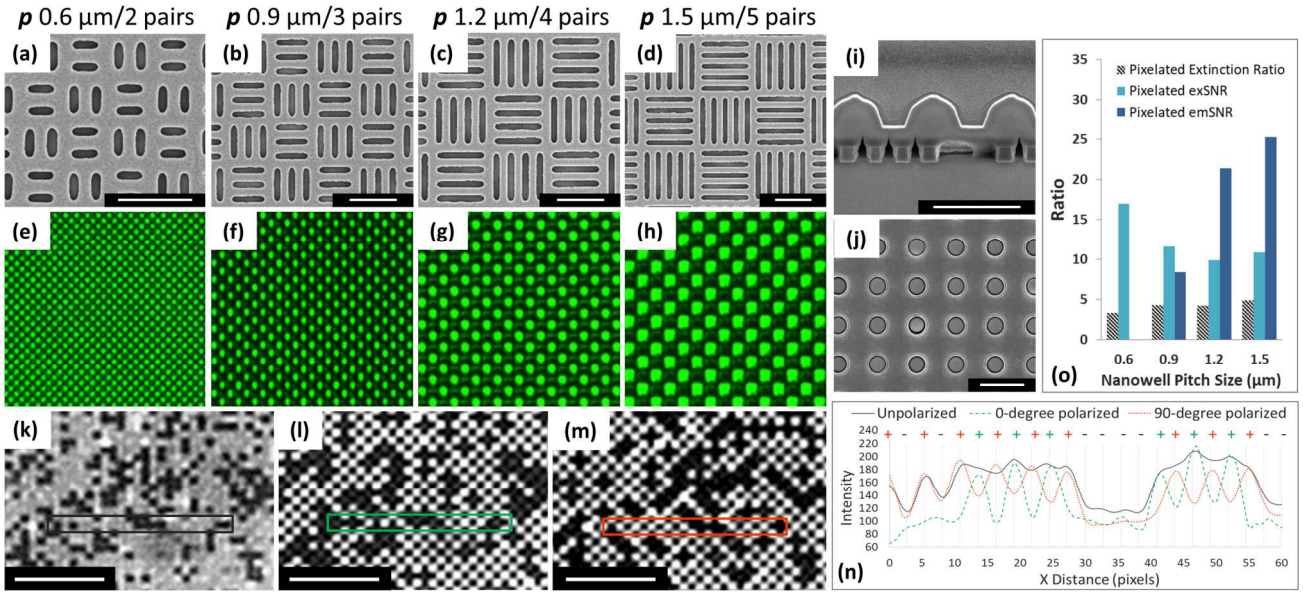

Fig. 4. Experimental results of the nanowell-based orthogonal nano/micropolarizer array biochip for resolution improvement *via* two imaging processes under 0-degree or 90-degree polarized excitation. (a)-(d) SEM images of the orthogonal nano/micropolarizer array with 2, 3, 4, and 5 pairs of 300-nm-period aluminum grating for nanowell pitch sizes of 0.6 μm, 0.9 μm, 1.2 μm, and 1.5 μm, respectively. (e)-(h) The excitation light distribution after a polarizer plate and an orthogonal nano/micropolarizer array at a transmission mode for nanowell pitch sizes of 0.6 μm, 0.9 μm, 1.2 μm, and 1.5 μm, respectively. (i) Cross-sectional SEM image of nanowell integrated on the orthogonal nano/micropolarizer array biochip, and (j) top-view SEM of the fluorescent-bead-loaded biochip. Fluorescence images of the fluorescent-bead-loaded biochip on a nanowell pitch size of 0.9 μm (k) without the polarizer plate, (l) with 0-degree polarizer plate, and (m) with 90-degree polarizer plate at a reflection mode. (n) The intensity profiles in the frames in (k)-(m). (o) The measured pixelated extinction ratio, excitation light signal-to-noise ratio (exSNR), and emission light signal-to-noise ratio (emSNR). Scale bar: 1 μm in (a)-(d), (i), and (j); 10 μm in (k)-(m)

polarizers at 0, 2.5, 5, 10, 15, 30, and 45 degrees was investigated to understand the alignment tolerances by the GSolver software (from Grating Solver Development Company (USA)). In Fig. 3, only when the leveling or rotation angle shifts larger than 10 degrees, the TM and TE transmittance present distinguishable differences. Thus, for practical usage, the insertion of a polarizer plate has to be calibrated with an alignment bias of smaller than 10 degrees in the optical microscope system.

III. Experimental Results

A. *Orthogonal nano/micropolarizer array and checkerboard excitation for superresolution imaging*

The top-view SEM images of the nano/micropolarizer array with pitch sizes of 0.6 μm, 0.9 μm, 1.2 μm, and 1.5 μm, respectively, were shown in Fig. 4(a)-(d). Although the corners of the grating nanostructures were rounding, the transmission and depression ability of the polarizer units with the 0-degree shift and the polarizer units with the 90-degree shift from the orientation of the excitation light polarizer plate was still sufficient (see the high contrast of the checkerboard excitation signals compared to the background in Fig. 4(e)-(h)). In Fig. 4(i)(j), the SEM images show the integration with nanowell array on the nano/microploarizer array and a maximum of one fluorescent bead loading in a nanowell. Fig. 4(k)-(m) demonstrate the resolution improvement based on the two-step imaging and a switchable checkerboard illumination. An unresolvable fluorescence image on a nanowell pitch size of 0.9 μm *via* nonpolarized excitation light and a 20X/NA0.5 objective (Fig. 4(k)) can be distinguished by first imaging *via* a 0-degree polarized excitation (Fig. 4(l)) and second imaging *via* a 90-degree polarized excitation (Fig. 4(m)). The intensity profiles in Fig. 4(n) agree with the phenomenon of resolution improvement that group signals become discrete PSFs after a checkerboard illumination. Fig. 4(o) quantifies the optical property of the pixelated nano/micropolarizer array for their extinction ratio, exSNR, and emSNR. The results show that the pixelated extinction ratio is higher than 3 which results in the exSNR and emSNR of 8~10. Although the emSNR at a pixel pitch of 0.6 μm was missing due to the failure of the nanowell integration on the 0.6 μm pitch, the pixelated extinction ratio and the pixelated exSNR still present a similar phenomenon to the other pixel pitches. Thus, we think a similar resolution improvement can still be achieved at the 0.6 μm pitch.

IV. Conclusions

This paper proposes a superresolution approach in another format for fluorescence signal detection in a nano/microarray, in which the optical system is compatible with conventional fluorescence microscopes, but additional integration of metal grating nanostructures on a transparent substrate is employed to generate a checkerboard excitation. Through two image captures, a √ 2-fold resolution improvement was demonstrated for a 0.9 μm nanowell pitch size. For smaller pitch sizes, eg. 400 nm, we think this concept can still be used as long as there are at least two grating pairs with a ⩽200-nm period that can be fabricated in one polarizer unit.

Acknowledgment

The authors thank Nanoelectronic Laboratory, Electronic and Optoelectronic System Research Laboratories (EOSL) of the Industrial Technology Research Institute (ITRI) for the fabrication of the nano/micropolarizer array chip.

REFERENCES

[1] Next Generation Sequencing and DNA Synthesis: Technology, Consumables Manufacturing and Market Trends 2019. Yole Developpement, April 2019.

[2] G. M. Skinner, G. W. EVANS, S. S. Hong, J. A. Moon, M. S. Bowen, J. M. Boutell, J. R. Betley, Super-resolution microscopy. US patent No. 10901230, Jan. 26, 2021.

[3] J. Tang, J. Ren, and K. Y. Han, "Fluorescence imaging with tailored light," Nanophotonics, 2019, 8, pp. 2111–2128.

[4] L. Schermelleh, A. Ferrand, T. Huser, C. Eggeling, M. Sauer, O. Biehlmaier, and G. P. C. Drummen, "Super-resolution microscopy demystified," Nat. Cell Biol., 2019, 21, pp.72–84.

[5] P. Li, G. Kang, I. Vartiainen, F. Wang, Y. Liu, and X. Tan, "Investigation of achromatic micro polarizer array for polarization imaging in visible-infrared band," Optik, 2018, 158, pp.1427–1435.

[6] H.-Y. Hsieh, C.-H. Lin, W.-K. Wang, and C.-C. Hsieh, ”Nanowell-based orthogonal submicropolarizer array biochip for multiple throughput of fluorescence sequencing," ACS Appl. Nano Mater., 2021, 4, pp.10409–10418.

[7] H.-Y. Hsieh, US Patent application No. 17/071,736, October 15, 2020.

[8] H.-Y. Hsieh, Y.-H. Peng, S.-F. Lin, L.-C. Chen, T.-C. Yu, C.-F. Chiou, and J. Lee "Triple-junction optoelectronic sensor with nanophotonic layer integration for single-molecule level decoding," ACS Nano, 2019, 13, pp.4486–4495.

[9] H.-Y Hsieh, T.-W. Huang, J.-L. Xiao, C.-S. Yang, C.-C. Chang, C.-C. Chu, L.-W. Lo, S.-H. Wang, P.-C. Wang, C.-C. Chieng, C.-H. Lee, and F.-G. Tseng "Fabrication and modification of dual-faced nano-mushrooms for tri-functional cell theranostics: SERS/fluorescence signaling, protein targeting, and drug delivery," J. Mater. Chem., 2012, 22, pp.20918–20928.

[10] H.-Y. Hsieh, P.-C. Wang, C.-L. Wu, C.-W. Huang, C.-C. Chieng, and F.-G. Tseng, "Effective enhancement of fluorescence detection efficiency in protein microarray assays: application of a highly fluorinated organosilane as the blocking agent on the background surface by a facile vapor-phase deposition process," Anal. Chem., 2009, 81, pp.7908–7916.